RESEARCH ARTICLE | JANUARY 18 2024

Radiation measurements at the WMO/CIMO testbed site Lindenberg FREE

Stefan Wacker ✉; Ralf Becker; Florian Filipitsch; Lionel Doppler

AIP Conf. Proc. 2988, 060022 (2024)
https://doi.org/10.1063/5.0183573

Radiation Measurements at the WMO/CIMO Testbed Site Lindenberg

Stefan Wacker[1, a)], Ralf Becker[1, b)], Florian Filipitsch[1, c)] and Lionel Doppler[1, d)]

[1]*Deutscher Wetterdienst, Meteorologisches Observatorium Lindenberg – Richard Aßmann Observatorium, Am Observatorium 12, D-15848 Tauche OT Lindenberg, Germany*

[a)] *Corresponding author: stefan.wacker@dwd.de*
[b)]*ralf.becker@dwd.de*
[c)]florian.filipitsch@dwd.de
[d)]lionel.doppler@dwd.de.

Abstract. The comprehensive radiation monitoring program comprising broadband, spectral and spectroscopic observations from the CIMO testbed site Lindenberg is presented. Long-term series of total solar and diffuse broadband radiation demonstrate the variations in the atmospheric transparency over the past 80 years such as the dimming in the 1950-1985 period followed by a continuous brightening. Total and direct shortwave radiation show significant trends at 3.5 and 9.3 Wm^{-2} per decade over the past 25 years, respectively. While the dimming and major parts of the brightening are most likely caused by variations in the aerosol optical depth, a possible decrease of the magnitude of the cloud radiative effect may contribute to the increase in solar radiation in the brightening period, especially in most recent years.

INTRODUCTION

The Meteorological Observatory Lindenberg – Richard Aßmann Observatory (MOL-RAO, 52.21° N, 14.12° E, 98 meters above sea level) of the German Meteorological Service (Deutscher Wetterdienst, DWD) is a WMO/CIMO testbed site with a comprehensive atmospheric observational program including in-situ and remotely sensed observations. MOL-RAO hosts the lead center of the Global Reference Upper Network (GRUAN) and a Regional and National Radiation Centre of the WMO, Region VI.

The radiation monitoring program includes broadband and spectral radiometry as well as spectroscopy. MOL-RAO is a station of the Baseline Surface Radiation Network (BSRN). Aerosol Optical Depth (AOD) and total column ozone have been observed since the mid-eighties using sunphotometers and the Brewer spectrometer, respectively. Nowadays, Precision Filter Radiometers (PFR), Cimel CE-318 and POM sunphotometers are used to observe AOD, column water vapor and optical properties of aerosols. The latter observations contribute to AERONET and the Euroskyrad (ESR) network, respectively, and have been upgraded to lunar operation mode for nighttime measurements. These observations are complemented by a star photometer to retrieve AOD and the total water vapor column during night. Two spectrometers from Bentham are used for UV observations and complemented by array-based spectrometers observing in the UV and from the UV into the near infrared. Finally, vertical profiles of incoming and outgoing shortwave and longwave radiation from the ground into the stratosphere are measured using radiosondes equipped with four component radiometers. These ascents are conducted at least once a month.

The long-term series of broadband solar radiation from the nearby Potsdam station belong to the longest records in the world and reflect the global dimming and brightening periods which have been widely discussed in the literature [1]. While the dimming and early brightening are caused by increasing and decreasing aerosol loads due to anthropogenic activities and the introduction of air pollution regulations, respectively, the causes for the recent increase are yet less understood. In this study, we focus on long-term series from the last 25 years, when reliable observations of the AOD and incoming longwave radiation are available. The latter allow the cloud radiative effect to be calculated and thus the contribution of aerosols and clouds to the observed trends to be determined.

Radiation Processes in the Atmosphere and Ocean
AIP Conf. Proc. 2988, 060022-1–060022-4; https://doi.org/10.1063/5.0183573
Published by AIP Publishing. 978-0-7354-4779-0/$30.00

METHODS

Observations

Operational observations of downwelling total solar (global, DSR) and diffuse radiation (DSR_{dif}) using thermopile-based pyranometers were initiated at MOL-RAO in 1981. At the nearby Potsdam observatory (approximately 80 km from MOL-RAO), the measurements were already started in 1937. For the observation of the diffuse component, a shadow band has been used. The Potsdam series have been homogenized including a transfer from various radiometric scales to the World Radiometric Reference (WRR) [2]. The sensors are exchanged and calibrated every second year. The two stations are manned and thus a reliable maintenance is available. These methods allow the solar radiation to be observed close to the instrument uncertainty at 2 % as stated by the manufacturer. In contrast to the solar radiation, the uncertainties in the observation of downwelling longwave radiation (DLR), which were initiated in 1991 and 1994 at Potsdam and Lindenberg, respectively, are considerably higher and data gaps more frequent. In fact, reliable observations of the longwave component are not available before the BSRN station was established in 1994. At the BSRN site, all incoming radiative fluxes are measured individually and redundantly. Apart from DSR, all radiation quantities are observed on solar trackers. The solar radiometers are calibrated in situ using absolute cavities whenever atmospheric conditions permit. Observations are within the uncertainties stated by BSRN, i.e. 0.5 % for the downwelling direct shortwave radiation (DSR_{dir}) and 2 % for DSR, DSR_{dif} and DLR.

Determination of the Cloud Radiative Effect

The cloud radiative effect (CRE) or total cloud radiative effect (TCE) is defined as the sum of the short- and longwave cloud effect (SCE and LCE) and is calculated as the difference of the all-sky broadband short- and longwave observations ($DSR_{obs,as}$; $DLR_{obs,as}$) and the corresponding hypothetical cloud-free fluxes, which would be expected at the same time in the absence of the clouds ($DSR_{cal,cf}$; $DLR_{cal,cf}$):

$$TCE = SCE + LCE = DSRobs,as - DSRcal,cf + DLRobs,as - DLRcal,cf \quad (1)$$

For the computation of the cloud-free shortwave irradiances, a pre-calculated lookup table was used providing the shortwave fluxes as a function of solar zenith angle, Integrated Water Vapor (IWV), and AOD. The lookup table had been compiled using the library for radiative transfer calculations, libRadtran [3] with the molecular absorption parameterization from LOWTRAN/SBDART [4]. The cloud-free long-wave fluxes were calculated using the empirical model of Dupont [5]. This parameterization uses screen-level temperature, IWV, a set of empirical corrections to account for the variations in the vertical temperature and humidity profiles, and four coefficients to calculate the longwave irradiance. The coefficients represent site-specific atmospheric conditions. A calibration data set was compiled containing cloud-free periods during day and night, which had been visually selected using images from a hemispherical sky camera. A second independent cloud-free data set was then used to validate the optimized model. The shortwave cloud-free model was validated with an extended cloud-free data set. Mean bias (MBE) and root mean squared error (RMSE) of the shortwave model was at -0.9 and 1.7 %, respectively. MBE and RMSE for the longwave cloud-free model was at 2.4 and 7.3 Wm^{-2} and thus the model uncertainties are slightly higher than the corresponding measurement uncertainties.

RESULTS AND DISCUSSION

Time series of DSR from Potsdam and MOL-RAO illustrate the decrease in the transparency of the atmosphere and thus the decrease of DSR at the surface from the 1950s (Fig. 1a). This decrease is commonly referred to as global dimming caused by an increase in the atmospheric aerosol load due to anthropogenic activities. The dimming period is followed by a brightening from the middle of the 1980s, i.e. an increase in DSR caused by a decrease in the aerosol load as a consequence of the implementation of air pollution mechanism. The decrease in the aerosol load is documented by the decrease in the AOD (Fig. 1b). The decrease in AOD at 500 nm between pre- and post-Pinatubo averages is approximately 40 %. For the post-Pinatubo period (from 1995 onwards) a weak negative trend of -0.0022 per year is observed. It has been shown that the decadal variations in DSR are most likely due to these human-induced modifications in the AOD, rather than changes in cloudiness [6]. However, it is unclear if the decrease in the direct aerosol effect can fully explain the most recent increase in solar radiation when the AOD was low and its decrease weak but the highest values in solar radiation were recorded.

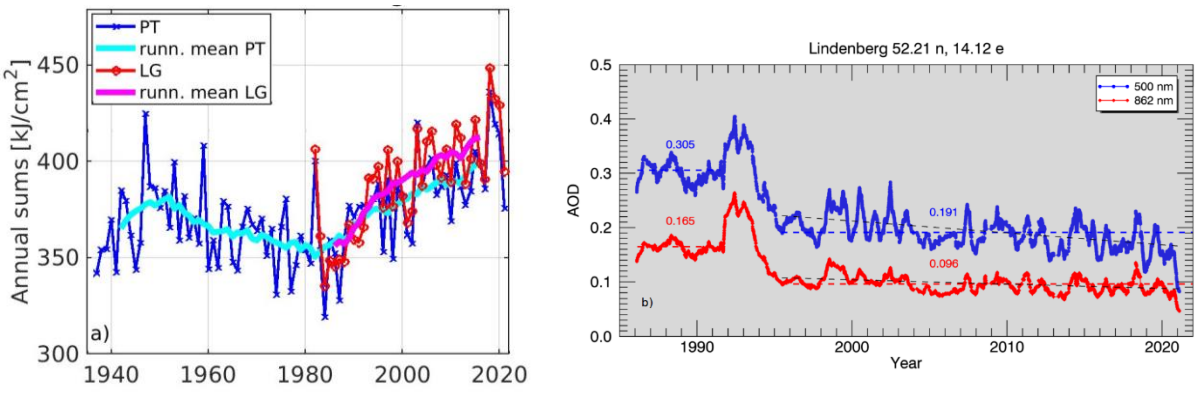

FIGURE 1. Annual sums and 10-year running mean of total solar radiation at Potsdam and MOL-RAO. The data stem from the ground network of DWD (panel (a)). 3-month running mean of the AOD at 500 and 862 nm at MOL-RAO. Numbers represent the respective averages of the pre- and post-Pinatubo periods (panel (b)).

For the 1996-2021 period, significant trends at 3.4 and 9.3 $Wm^{-2}dec^{-1}$ for DSR and DSR_{dir} are observed, respectively (Table 1). The highest trends occur in spring and summer, while they are considerably smaller and not significant in fall and winter. DSR_{dif} has insignificantly decreased by -2.2 ± 2.5 Wm^{-2} since 1996, an indication of reduced scattering. To study the causes for the observed radiation trends, a cloud-free dataset was compiled using the automatic DWD cloud algorithm, which is based on ceilometer observations and thus can be used during day and night, i.e. also for the longwave. However, the observed cloud-free trends in the shortwave are up to four times higher than the respective all-sky trends and thus not reasonable. Indeed, radiative transfer calculations indicate that the observed decrease in AOD of 25 % for the 1996-2021 period should result in an increase of about 9 and 18 Wm^{-2} for DSR and DSR_{dir}, respectively. Since humidity and total column ozone have not changed significantly, such high

TABLE 1. Slope of decadal (10 years) all-sky trends including lower and upper confidence bounds at the 95 % level for the 1996-2021 period at MOL-RAO. Significant trends are in bold. Unit for specific humidity q is (g H_2O (gas)/kg wet air) dec^{-1}. All radiation data stem from the BSRN station.

Parameter	Trend				
	Spring (MAM)	Summer (JJA)	Fall (SON)	Winter (DJF)	Year
DSR [$Wm^{-2}dec^{-1}$]	4.8 [-1.7, 11.4]	**7.4 [1.1, 13.8]**	1.5 [-2.8, 5.8]	-0.2 [-1.7, 1.3]	**3.4 [0.3, 6.6]**
DSR_{dir} [$Wm^{-2}dec^{-1}$]	12.8 [-2.0, 27.6]	**19.2 [7.8, 30.5]**	6.6 [-4.7, 17.8]	-1.4 [-7.0, 4.3]	**9.3 [2.2, 16.3]**
DSR_{dif} [$Wm^{-2}dec^{-1}$]	-0.7 [-3.2, 1.8]	**-2.3 [-4.1, -0.5]**	-0.5 [-1.6, 0.6]	0.2 [-0.8, 1.1]	-0.8 [-1.8, 0.1]
DLR [$Wm^{-2}dec^{-1}$]	0.6 [-2.3, 3.6]	**4.7 [3.2, 6.2]**	**4.2 [1.4, 7.0]**	**5.4 [1.9, 9.0]**	**3.8 [2.3, 5.3]**
T_{2m} [°Cdec^{-1}]	0.3 [-0.3, 1.0]	**0.9 [0.4, 1.4]**	**0.8 [0.2, 1.3]**	0.8 [-0.3, 1.8]	**0.7 [0.3, 1.1]**
q	-0.2 [-0.4, 0.0]	-0.2 [-0.2, 0.2]	0.1 [-0.1, 0.3]	0.1 [-0.1, 0.3]	0.0 [-0.1, 0.1]

positive cloud-free trends cannot be explained by the AOD decrease and hence they are not reasonable. It is possible that the cloud-free dataset is contaminated by clouds and their variations may have increased the observed trends. A pure zenithal cloud detection algorithm may therefore not be suitable for such an application.

Regarding the all-sky DLR, a positive and significant trend at 3.8 $Wm^{-2}dec^{-1}$ is observed. This increase is consistent with projections from General Circulations Models (GCM) and is most likely caused by a significant air temperature (T_{2m}) increase at 2.2 ± 2.5 Wm^{-2} since 1996 and increasing greenhouse gas concentrations.

The CRE was calculated according to Equation 1. The SCE is always negative and its magnitude is lower during winter due to the reduced number of day light hours (Fig. 2a). Annual mean SCE is -60 Wm^{-2}. On the other hand, the LCE is always positive and higher during the winter months due to higher occurrence of low-level clouds such as stratus (fog) and lower water vapor content. Mean annual LCE is 30 Wm^{-2}. The TCE is dominated by the SCE and hence negative during most of the year except in November, December and January when the TCE is positive at 20 Wm^{-2} due to the reduced SCE. Mean annual TCE is – 30 Wm^{-2}. A positive but not significant trend of 1.8 $Wm^{-2}dec^{-1}$ is observed for the SCE, which represents a decrease in the magnitude of the SCE (Fig. 2b). This decrease may be caused by a decrease in cloud cover, shift towards a different cloud type and/or changes in microphysical cloud properties. The LCE trend is positive and significant at 1.6 $Wm^{-2}dec^{-1}$. In contrast to a positive SCE trend, a positive LCE trend implies an increase in cloudiness. Possible explanations for this apparent contradiction include uncertainties in the cloud-free models and changes in cloud properties or atmospheric parameters which may affect the SCE and

LCE differently. For instance, the decrease in the magnitude of the SCE could be caused by a decrease in cloud optical thickness and changes in the cloud phase without a decrease in cloud fraction. The LCE, on the other hand, could be caused by changes in atmospheric and cloud base temperatures, cloud base height, cloud opacity and other cloud properties. To fully explain the trends in the CRE, ancillary observations of such macro- and microphysical cloud properties need to be included in future analysis. Finally, the trend of the TCE is positive at 3.5 $Wm^{-2}dec^{-1}$ and significant at the 95 % level. The positive value of the TCE trend represents an overall decrease in the TCE magnitude and indicates that changes in cloud properties have most likely occurred during the 1996–2021 period and thus contributed to the increase in solar radiation.

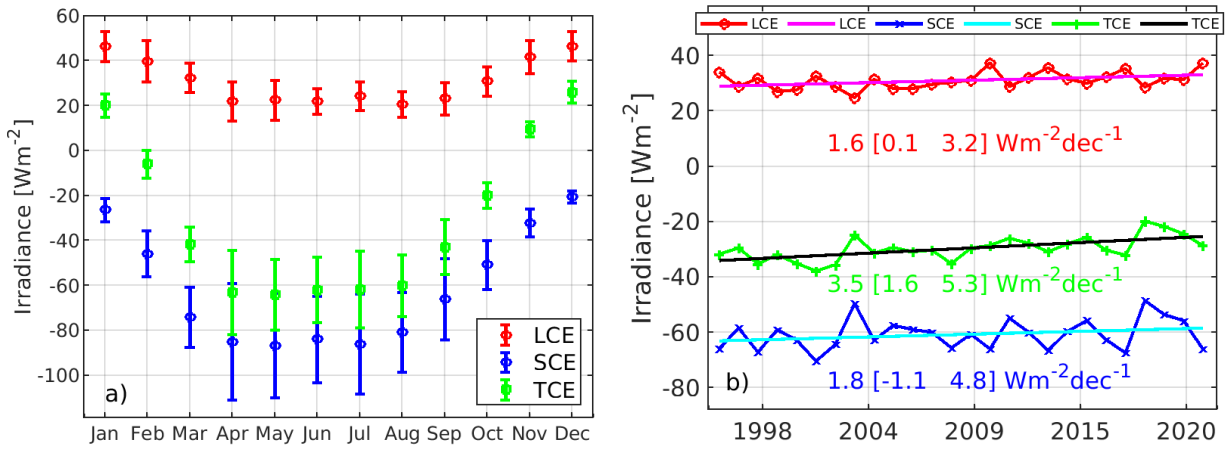

FIGURE 2. Annual course of the shortwave (SCE), longwave (LCE) and total cloud effect (TCE) at MOL-RAO (panel (a)). Error bars are given as standard deviations calculated from the 1996-2021 period. Corresponding annual means with trend line are shown in panel (b). Lower and upper confidence bounds of the slopes are given at the 95 % level (in brackets).

CONCLUSION

MOL-RAO has a comprehensive observational radiation program including broadband shortwave and longwave radiation, spectral and spectroscopic observations from the UV over the visible into the near infrared and measurements of radiation profiles from the ground into the stratosphere. In the broadband shortwave radiation, a continuous brightening after the dimming period (1950-1985) is observed. Total and direct shortwave radiation have increased since 1996 by 10 and 25 Wm^{-2}, respectively. The increase in incoming longwave radiation is at 10 Wm^{-2}, mainly caused by raising air temperature and greenhouse gas concentrations and is in line with the output of GCM's. While the long-term variations in shortwave radiation over the past 80 years can be explained by changes in the direct aerosol effect, it is most likely that a decrease in the magnitude of the cloud radiative effect has contributed to the recent increase. However, the interpretation of the trends in the cloud radiative effect is not conclusive and hence the analysis of observations of macro- and microphysical cloud properties is necessary.

REFERENCES

1. M. Wild, "Global dimming and brightening: A review," J. Geophys. Res **114**, (2009).
2. K. Behrens, "Recording of solar radiation components for 75 years in Potsdam (Germany). AIP Conference Proceedings, **1531**, 548-551 (2013).
3. C. Emde, R. Buras-Schnell, A. Kylling, B. Mayer, J. Gasteiger, U. Hamann, et al. "The libRadtran software package for radiative transfer calculations (version 2.0.1)," Geosci. Model Dev., ***9***(5), 1647–1672 (2016).
4. P. Ricchiazzi, S. Yang, C. Gautier, and D. Sowle. SBDART: A research and Teaching software tool for plane-parallel radiative transfer in the Earth's atmosphere," Bull. Amer. Meteor. Soc, **79**, 2101–2114 (1998).
5. J-Ch. Dupont, M. Haeffelin, P. Drobinski and T. Besnard, „Parametric model to estimate clear-sky longwave irradiance at the surface on the basis of vertical distribution of humidity and temperature," J. Geophys. Res., **113**, (2008).
6. M. Wild, S. Wacker, S. Yang, and A. Sanchez-Lorenzo, "Evidence for Clear-Sky Dimming and Brightening in Central Europe," Geophys. Res. Lett. **48**, (2021).